

# SENSITIVITY ANALYSIS OF THE LWR MODEL FOR TRAFFIC FORECAST ON LARGE NETWORKS USING WASSERSTEIN DISTANCE

MAYA BRIANI

*Istituto per le Applicazioni del Calcolo “M. Picone”,  
Consiglio Nazionale delle Ricerche  
Via dei Taurini, 19  
00185 Rome, Italy  
m.briani@iac.cnr.it*

EMILIANO CRISTIANI

*Istituto per le Applicazioni del Calcolo “M. Picone”,  
Consiglio Nazionale delle Ricerche  
Via dei Taurini, 19  
00185 Rome, Italy  
e.cristiani@iac.cnr.it*

ELISA IACOMINI

*Dipartimento di Matematica  
Sapienza – Università di Roma  
P.le Aldo Moro, 5  
00185 Roma, Italy*

In this paper we investigate the sensitivity of the LWR model on network to its parameters and to the network itself. The quantification of sensitivity is obtained by measuring the Wasserstein distance between two LWR solutions corresponding to different inputs. Hence, we propose a numerical method to approximate the Wasserstein distance between two density distributions defined on a network. We found a large sensitivity to the traffic distribution at junctions, the network size, and the network topology.

*Keywords:* LWR model; networks; traffic; uncertainty quantification; Wasserstein distance; earth mover’s distance; Godunov scheme; multi-path model; linear programming.

2010 AMS Subject Classification: 35R02, 35L50, 90B20, 90C05

## 1. Introduction

In this paper we deal with the sensitivity analysis of the celebrated LWR model for traffic forecast on networks. The LWR model was introduced by Lighthill and Whitham<sup>21</sup> and Richards,<sup>24</sup> and it paved the way to the macroscopic description of traffic flow.<sup>1,16,17</sup> In such a macroscopic models, traffic is described in terms of average density  $\rho = \rho(x, t)$  and velocity  $v = v(x, t)$  of vehicles, rather tracking each single vehicle. The natural assumption that the total mass is conserved along the

road leads to impose that  $\rho$  and  $v$  obey

$$\partial_t \rho + \partial_x(\rho v) = 0, \quad \rho(x, 0) = \rho^0(x) \quad (1.1)$$

for  $(x, t) \in \mathbb{R} \times [0, T]$ , a final time  $T > 0$ , and initial distribution  $\rho^0$ . In first-order models like LWR, the velocity  $v = v(\rho)$  is given as function of the density  $\rho$ , thus closing the equation. In the rest of the paper we will assume that the maximal density of vehicles is normalized to 1 and the fundamental diagram  $f(\rho) := \rho v(\rho)$  has the form

$$f(\rho) := \begin{cases} \frac{f_{\max}}{\sigma} \rho, & \text{if } \rho \leq \sigma \\ \frac{f_{\max}}{\sigma-1}(\rho-1), & \text{if } \rho > \sigma \end{cases} \quad (1.2)$$

for some  $\sigma \in (0, 1)$  and  $f_{\max} > 0$ , see Fig. 1.

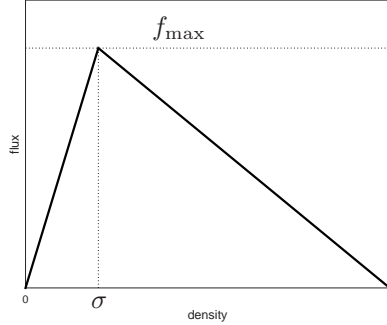


Fig. 1. Fundamental diagram  $f(\rho) = \rho v(\rho)$ .

In order to describe real situations where the vehicles move on several interconnected roads, the simple model (1.1) is not sufficient. This has motivated several authors to consider analogous equations on a network (metric graph), which is a directed graph whose edges are equipped with a system of coordinates. In this context vertices are called *junctions* and edges are called *roads*. The natural way to extend (1.1) to a network is to assume that the conservation law is separately satisfied on each road for all times  $t > 0$ . Moreover, additional conditions have to be imposed at junctions, because in general the conservation of the mass alone is not sufficient to characterize a unique solution. We refer the reader to the book by Garavello and Piccoli<sup>14</sup> for more details about the ill-posedness of the problem at junctions. Multiple workarounds for such ill-posedness have been suggested in the literature: (i) maximization of the flux across junctions and introduction of priorities among the incoming roads<sup>6,14,20</sup>; (ii) introduction of a *buffer* to model the junctions by means of additional ODE coupled with (1.1)<sup>3,13,15,18</sup>; (iii) reformulation of the problem on all possible paths on the network rather than on roads and junctions.<sup>4,5,19</sup> In general, they all allow to determine a unique solution for the traffic evolution on the network, but the solutions might be different.

In the following we will employ the latter approach together with a Godunov-based numerical approximation,<sup>4,5</sup> also used to reproduce Wardrop equilibria.<sup>8</sup> More recently, it was shown that the solution computed by the path-based model coincides with the many-particle limit of the first-order microscopic follow-the-leader model.<sup>9</sup>

In this paper we aim at quantifying the sensitivity of the LWR model to its inputs. In particular we will focus on the following inputs:

- initial datum;
- fundamental diagram;
- traffic distribution at junctions;
- network size;
- network connectivity.

The sensitivity will be measured by computing the distance between two LWR solutions obtained with different inputs or parameters, in order to understand their impact on the final solution. The question arises which distance is more suitable to this kind of investigation. It is by now well understood that  $L^p$  distances do not catch the natural concept of distance among densities, see, e.g., the discussion in Ref. 7 (Sec. 7.1) and Sec. 3 in this paper. A notion of distance which instead appears more natural is that of *Wasserstein distance*, see, e.g., Refs. 2, 7, 10, 12, 23. The bottleneck for using this distance on networks comes from the computational side. In fact, the classical definition of Wasserstein distance is not at all suitable for numerical approximation. It is therefore necessary to find an alternative definition or method to compute it. Here we propose an algorithm to approximate the Wasserstein distance on a network, keeping within the limits complexity and CPU time.

To the knowledge of the authors, the study presented here is the first one employing the Wasserstein distance to quantify the sensitivity of a macroscopic model for traffic flow on networks.

### *Paper organization*

In Sec. 2 we present in detail the mathematical model, which is a local version of the path-based approach,<sup>4,5</sup> suitable to deal with large networks. In Sec. 3 we motivate the choice of the Wasserstein distance for the subsequent sensitivity analysis and we review several ways to define and numerically compute it. This section is also meant to promote further investigations, comparisons and novel numerical methods in order to speed up the computation. In Sec. 4, which is the core of the paper, we present several tests designed to show the sensitivity of the model to various parameters and inputs. Finally, in Sec. 5 we sketch some conclusions.

## 2. A path-based model for large networks

In this section we introduce the network and the model we will use in the following to describe the traffic flow.

### 2.1. Basic definitions: graph vs. network and computational grid

Let us consider a connected and directed graph  $\mathcal{G} = (\mathcal{E}, \mathcal{V})$  consisting of a finite set of vertices  $\mathcal{V}$  and a set of oriented edges  $\mathcal{E}$  connecting the vertices.

Stemming from  $\mathcal{G}$ , we build the network  $\mathcal{N}$  by assigning to each edge  $E \in \mathcal{E}$  a positive length  $L_E \in (0, +\infty)$ . Moreover, a coordinate is assigned to each point of the edge. The coordinate will be denoted by  $x_E$  and it increases accordingly to the direction of the edge, i.e. we have  $x_E = 0$  at the initial vertex and  $x_E = L_E$  at the terminal vertex.

For numerical purposes, the network has to be discretised by means of a grid. Let us denote by  $\Delta x$  the space step. To avoid technicalities, let us assume that the length of all the edges is a multiple of  $\Delta x$  so that we can easily use the same grid size everywhere in  $\mathcal{N}$ . In this way, each edge is being divided in  $J_E := \frac{L_E}{\Delta x}$  cells. The total number of cells in  $\mathcal{N}$  is  $J := \sum_{E \in \mathcal{E}} J_E$ . The centre of each cell on edge  $E$  will be denoted by  $x_{E,j}$ ,  $j = 1, \dots, J_E$ , and the cell itself by  $C_{E,j} = [x_{E,j-\frac{1}{2}}, x_{E,j+\frac{1}{2}}]$ .

Finally, let us denote by  $\Delta t$  the time step. The number of time iterations will be denoted by  $N_T := \frac{T}{\Delta t}$ .

### 2.2. The model

In Refs. 4, 5 it was introduced a Godunov-based numerical algorithm to solve the LWR equations on small networks. The problem is reformulated on (possibly overlapping) paths joining all possible sources with all possible destinations, see Fig. 2. Let us denote by  $n_p$  the total number of paths on  $\mathcal{N}$ . Rather than tracking the total

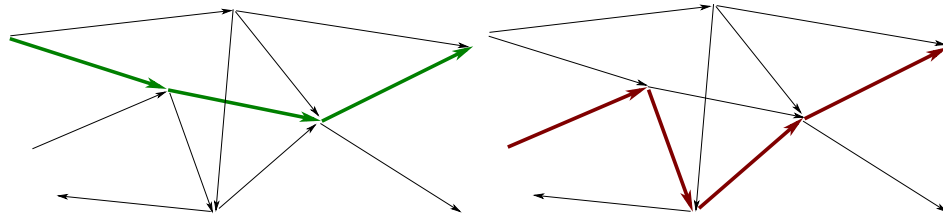


Fig. 2. A generic network. Two possible paths are highlighted. Note that the two paths share an arc of the network.

density  $\rho$ , one defines subdensities  $\mu^p$ ,  $p = 1 \dots, n_p$ , each of which represents the amount of vehicles following the  $p$ -path. Clearly the dynamics of vehicles following the  $p$ -path are influenced by those of vehicles following other paths whenever

the two populations share the same portion of the network. From the mathematical point of view, the problem is formulated as a system of  $n_p$  conservation laws with discontinuous flux and no special treatment of the junction is needed (each path is seen as an uninterrupted road). The main drawback of this approach is that the number of paths grows exponentially with the size of the network and the system becomes rapidly unmanageable. In Refs. 4, 5 it was also suggested a hybrid approach which keeps within the limits the computational effort, but it was not detailed. In the following we fill the gap giving the precise algorithm and testing it on real-size networks.

Define as usual the unknown density at grid nodes as

$$\rho_{E,j}^n := \frac{1}{\Delta x} \int_{x_{E,j-\frac{1}{2}}}^{x_{E,j+\frac{1}{2}}} \rho(y, n\Delta t) dy, \quad E \in \mathcal{E}, \quad j = 1, \dots, J_E, \quad n = 1, \dots, N_T.$$

Starting from the initial condition  $\rho_{E,j}^0 := \frac{1}{\Delta x} \int_{x_{E,j-\frac{1}{2}}}^{x_{E,j+\frac{1}{2}}} \rho^0(y) dy$ , the approximate solution at any internal cell  $j = 2, \dots, J_E - 1$  of any edge  $E \in \mathcal{E}$  is easily found by the standard Godunov scheme

$$\rho_{E,j}^{n+1} = \rho_{E,j}^n - \frac{\Delta t}{\Delta x} \left( G(\rho_{E,j}^n, \rho_{E,j+1}^n) - G(\rho_{E,j-1}^n, \rho_{E,j}^n) \right), \quad n = 0, \dots, N_T - 1, \quad (2.1)$$

where the numerical flux  $G$  is defined as

$$G(\rho_-, \rho_+) := \begin{cases} \min\{f(\rho_-), f(\rho_+)\} & \text{if } \rho_- \leq \rho_+ \\ f(\rho_-) & \text{if } \rho_- > \rho_+ \text{ and } \rho_- < \sigma \\ f(\sigma) & \text{if } \rho_- > \rho_+ \text{ and } \rho_- \geq \sigma \geq \rho_+ \\ f(\rho_+) & \text{if } \rho_- > \rho_+ \text{ and } \rho_+ > \sigma \end{cases}. \quad (2.2)$$

Around vertices we proceed as follows: let us focus on a generic vertex  $v \in \mathcal{V}$  and denote by  $n_{\text{inc}}^v$  and  $n_{\text{out}}^v$  the number of incoming and outgoing edges at  $v$ , respectively. As in the classical approaches,<sup>14</sup> we assume that it is given a traffic distribution matrix  $A^v = (\alpha_{R'R}^v)$ ,  $R = 1, \dots, n_{\text{inc}}^v$ ,  $R' = 1, \dots, n_{\text{out}}^v$  which prescribes how the traffic distributes in percentage from any incoming edge  $R$  to any outgoing edge  $R'$ . Clearly  $0 \leq \alpha_{R'R}^v \leq 1 \ \forall R, R'$  and  $\sum_{R'} \alpha_{R'R}^v = 1 \ \forall R$ .

Now, following the path-based approach, we look at all the possible paths across the vertex  $v$ . Having  $n_{\text{inc}}^v$  incoming edges and  $n_{\text{out}}^v$  outgoing edges, we have  $n_p^v := n_{\text{inc}}^v \times n_{\text{out}}^v$  possible paths. We denote by  $\mu_{E,j}^n(p, v)$  the density of the vehicles in the cell  $j$  of edge  $E$  at time  $t^n$  moving along path  $p$  across vertex  $v$ .

Let us now focus on a generic path  $p = (E, E')$  which joins edge  $E$  with  $E'$ , see Fig. 3. At  $t = 0$ , we set the value of  $\mu(p, v)$  at the last cell of the incoming edge by resorting to the matrix  $A$ ,

$$\mu_{E,J_E}^0(p, v) = \alpha_{EE'}^v \rho_{E,J_E}^0. \quad (2.3)$$

Instead, at the first cell of the outgoing edge we can split the total density in equal parts, being the correct subdensity unknown and noninfluential after a short

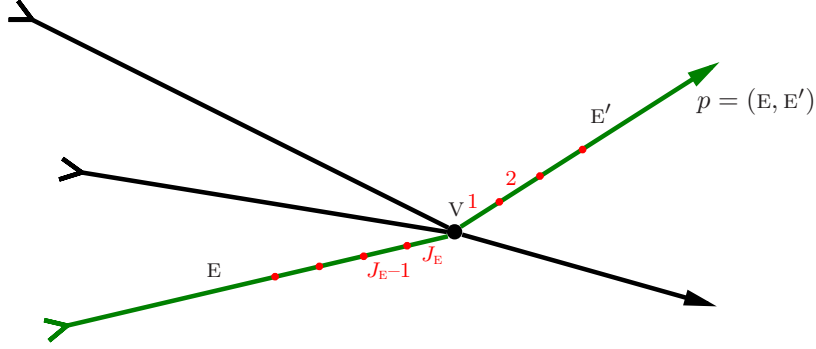


Fig. 3. The part of the network around the vertex  $v$ . Path  $p = (E, E')$  is drawn in green. Cells' labels are drawn in red.

transient,

$$\mu_{E',1}^0(p, v) = \frac{\rho_{E',1}^0}{n_{\text{inc}}^v}. \quad (2.4)$$

At this point we are ready to apply the Godunov-based multi-path scheme<sup>4,5</sup> with minor modifications for all paths of all vertices. Dropping the indices  $p$  and  $v$  for readability, we have in the last cell of the incoming edge:

$$\mu_{E,J_E}^{n+1} = \mu_{E,J_E}^n - \frac{\Delta t}{\Delta x} \left( \frac{\mu_{E,J_E}^n}{\rho_{E,J_E}^n} G(\rho_{E,J_E}^n, \rho_{E',1}^n) - \alpha_{EE'}^V G(\rho_{E,J_E-1}^n, \rho_{E,J_E}^n) \right), \quad (2.5)$$

for  $n = 0, \dots, N_T - 1$ . Note the presence of the parameter  $\alpha_{EE'}^V$  in front of the incoming flux which tells that only a percentage of the total mass is following path  $p$ .

In the first cell of the outgoing edge we have instead:

$$\mu_{E',1}^{n+1} = \mu_{E',1}^n - \frac{\Delta t}{\Delta x} \left( \frac{\mu_{E',1}^n}{\rho_{E',1}^n} G(\rho_{E',1}^n, \rho_{E',2}^n) - \frac{\mu_{E,J_E}^n}{\rho_{E,J_E}^n} G(\rho_{E,J_E}^n, \rho_{E',1}^n) \right), \quad (2.6)$$

for  $n = 0, \dots, N_T - 1$ .

Finally, let us note that at any time step the subdensities  $\mu$ 's must be summed (where defined) to recover the total density  $\rho$ , to be used at the next time step in (2.1), (2.5), and (2.6).

### 3. Wasserstein distance

It is well known that several problems in traffic modelling require the comparison of two density functions representing traffic conditions. In the following we list some of them:

- theoretical study of properties of the solution of scalar conservation laws;

- convergence of the numerical schemes (verifying that the numerical solution is close to the exact solution);
- calibration (finding the values of the parameters for the predicted outputs to be as close as possible to the observed ones);
- validation (checking if the outputs are close to the observed ones);
- sensitivity analysis (quantifying how the uncertainty in the outputs can be apportioned to different sources of uncertainty in the inputs and/or model's parameters). This is the problem we consider in this paper.

In this section we introduce the Wasserstein distance<sup>a</sup> as the main ingredient for the quantification of the distance between two outputs of the LWR model (e.g., density, velocity, flux).

### 3.1. Motivations and definitions

In many papers the quantification of the closeness of two outputs is performed by means of the  $L^1$ ,  $L^2$  or  $L^\infty$  distance (in space at final time or in both space and time). Although this can be satisfactory for nearly equal outputs or for convergence results, it appears inadequate for measuring the distance of largely different outputs. To see this, let us focus on the density of vehicles. In Fig. 4 three density functions

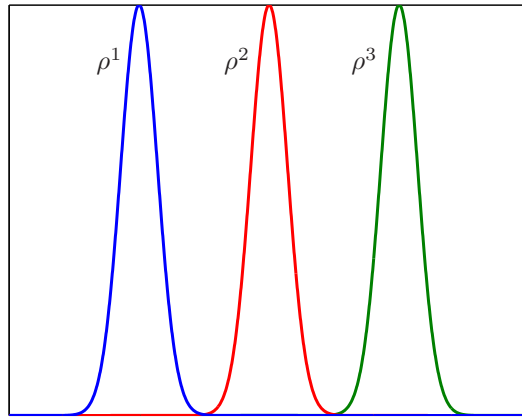


Fig. 4.  $L^p$  distance vs. Wasserstein distance.

$\rho^i$ ,  $i = 1, 2, 3$ , corresponding to the same total mass, say  $M$ , are plotted. It is plain that the  $L^1$  distances between  $\rho_1$  and  $\rho_2$  and between  $\rho_1$  and  $\rho_3$  are both equal to

<sup>a</sup>The Wasserstein distance was first introduced by Kantorovich in 1942 and then rediscovered many times. Nowadays, it is also known as *Lip'*-norm, earth mover's distance,  $\bar{d}$ -metric, Mallows distance. An important characterization is also given by the Kantorovich–Rubinstein duality theorem.

$2M$ . Similarly, all  $L^p$  distances are blind with respect to variation of the densities once the supports of them are disjoint. Our perception of distance is instead better caught by the Wasserstein distance as we will see in the following.

Let us denote by  $(X, \mathfrak{D})$  a complete and separable metric space, and by  $\mathcal{B}(X)$  a Borel  $\sigma$ -algebra of  $(X, \mathfrak{D})$ . Let us also denote by  $\mathcal{M}^+(X)$  the set of non-negative finite Radon measures on  $(X, \mathcal{B}(X))$ . Let  $\nu^s$  and  $\nu^d$  be two Radon measures in  $\mathcal{M}^+(X)$  such that  $\nu^s(X) = \nu^d(X)$ .

**Definition 3.1 (Wasserstein distance).** For any  $q \in [1, +\infty)$ , the  $L^q$ -Wasserstein distance between  $\nu^s$  and  $\nu^d$  is

$$W_q(\nu^s, \nu^d) := \left( \inf_{\gamma \in \Gamma(\nu^s, \nu^d)} \int_{X \times X} \mathfrak{D}(x, y)^q d\gamma(x, y) \right)^{1/q} \quad (3.1)$$

where

$$\begin{aligned} \Gamma(\nu^s, \nu^d) := \\ \left\{ \gamma \in \mathcal{M}^+(X \times X) \text{ s.t. } \gamma(A \times X) = \nu^s(A), \gamma(X \times B) = \nu^d(B), \forall A, B \subset X \right\}. \end{aligned}$$

Assuming that the measures  $\nu^{\{s, d\}}$  are absolutely continuous with respect to the Lebesgue measure, i.e. there are two density functions  $\rho^{\{s, d\}}$  such that  $d\nu^{\{s, d\}} = \rho^{\{s, d\}} dx$ , and considering the particular case  $X = \mathbb{R}^n$ ,  $\mathfrak{D}(x, y) = \|x - y\|_{\mathbb{R}^n}$ , we have

$$W_q(\nu^s, \nu^d) = W_q(\rho^s, \rho^d) = \left( \inf_{T \in \mathcal{T}} \int_{\mathbb{R}^n} \|T(x) - x\|_{\mathbb{R}^n}^q \rho^s(x) dx \right)^{1/q} \quad (3.2)$$

where

$$\mathcal{T} := \left\{ T : \mathbb{R}^n \rightarrow \mathbb{R}^n \text{ s.t. } \int_A \rho^d(x) dx = \int_{\{x: T(x) \in A\}} \rho^s(x) dx, \quad \forall A \subset \mathbb{R}^n \text{ bounded} \right\}.$$

Definition (3.2) sheds light on the physical interpretation of the Wasserstein distance, putting it in relation with the well known Monge–Kantorovich mass transfer problem<sup>27</sup>: a pile of, say, soil, with mass density distribution  $\rho^1$ , has to be moved to an excavation with mass density distribution  $\rho^2$  and same total volume. Moving a unit quantity of mass has a cost which equals the distance between the source and the destination point. We consequently are looking for a way to rearrange the first mass onto the second which requires minimum cost.

**Remark 3.1.** In our framework, the mass to be moved corresponds to that of vehicles. Since we are considering macroscopic models, vehicles are indistinguishable and we are not able to measure the distance of the *same* vehicle in the two scenarios. Therefore, we are measuring the distance between two vehicle densities by computing the minimal cost needed to superimpose vehicles in one scenario onto vehicles in another scenario. Moreover, we assume that the mass transfer *is constrained to happen along the network  $\mathcal{N}$*  (i.e.  $X = \mathcal{N}$ ), but the transfer *does not need to respect*

usual road laws (road direction, traffic distribution at junctions, etc.). This is reasonable since the measure of the error is conceptually different from the physical motion of vehicles.

Note that if we consider two concentrated measures  $\nu^s = \delta_x$  and  $\nu^d = \delta_y$ , the Wasserstein distance between the two is  $W_q(\delta_x, \delta_y) = |x - y|$ , as one would expect. This is also the desired distance quantification in the case of only two vehicles on a road, located in  $x$  and  $y$  respectively.

Unfortunately, definitions (3.1) and (3.2), though elegant, are not suitable for numerical approximation. Limiting our attention to the real line, the problem is easily solved by using nice alternative definitions of Wasserstein distance, like the ones reported in the following.

If  $q = 1$ , we have

$$W_1(\rho^s, \rho^d) = \int_{\mathbb{R}} |F^s(x) - F^d(x)| dx, \quad F^{\{s,d\}}(x) := \int_{-\infty}^x \rho^{\{s,d\}}(x) dx. \quad (3.3)$$

If  $q = 2$ , we have

$$W_q(\rho^s, \rho^d) = \left( \int_X |T^*(x) - x|^2 \rho^s(x) dx \right)^{1/2} \quad (3.4)$$

where  $T^*$  is easily found as the function that satisfies

$$\int_{y < T^*(x)} \rho^d(y) dy = \int_{y < x} \rho^s(y) dy, \quad \forall x \in \mathbb{R}.$$

The case of a network is more complicated. In the following section we propose an algorithm to approximate the Wasserstein distance on a network, reformulating the problem on a discrete graph.

### 3.2. Hitchcock's discrete formulation on graphs

A network can be always approximated by a discrete graph at the cost of a loss of resolution. Resorting to the discretisation introduced in Sec. 2.1, we can create a new, undirected graph whose vertices coincide with the centres of the cells, and they are connected in agreement with the network, see Fig. 5. The graph created by this procedure will be denoted hereafter by  $\mathcal{G}_N^\Delta$ . The number of vertices of  $\mathcal{G}_N^\Delta$  equals the total number of cells in  $\mathcal{N}$ , therefore will be denoted by  $J$ . In order to complete the discretisation procedure, *the mass distributed on each cell is accumulated to the vertex located at the centre of the cell*. Doing this, the problem is reformulated as an optimal mass transportation problem on a graph. The new problem clearly approximates the original one on the network  $\mathcal{N}$  and the approximation error is controlled by  $\Delta x$ . In the following we will give a precise estimate.

At this point one can resort to classical methods, see e.g. Chapt. 19 in Ref. 25 and references therein, recasting the problem in the framework of *linear programming* (LP).

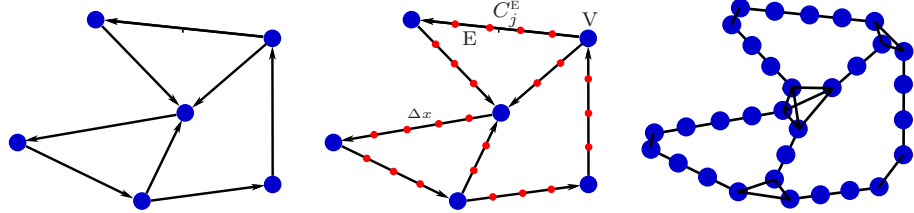


Fig. 5. Original directed graph  $\mathcal{G}$  (left), network  $\mathcal{N}$  built on  $\mathcal{G}$  discretised with space step  $\Delta x$  (centre), and undirected graph  $\mathcal{G}_N^\Delta$  built on the discretised network  $\mathcal{N}$  (right).

Let us enumerate the vertices of  $\mathcal{G}_N^\Delta$  by  $j = 1, \dots, J$ , and denote by  $\rho_j^S, \rho_j^D$ , the supply and demand densities concentrated in vertex  $j$ , respectively. Following the mass transport interpretation, the supply mass at vertex  $j$  is  $s_j := \rho_j^S \Delta x$ , and the demand mass is  $d_j := \rho_j^D \Delta x$ . Let  $c_{jk}$  be the cost of shipping a unit quantity of mass from the origin  $j \in \{1, \dots, J\}$  to the destination  $k \in \{1, \dots, J\}$ . Here we define  $c_{jk}$  as the length of the shortest path joining  $j$  and  $k$  on  $\mathcal{G}_N^\Delta$ , which can be easily found by, e.g., the Dijkstra algorithm. Let  $x_{jk}$  be the quantity shipped from the origin  $j$  to the destination  $k$ . The problem is then formulated as

$$\begin{aligned} \text{minimize} \quad & \mathcal{H} := \sum_{j=1}^J \sum_{k=1}^J c_{jk} x_{jk} \\ \text{subject to} \quad & \sum_k x_{jk} = s_j, \quad \forall j \\ & \sum_j x_{jk} = d_j, \quad \forall k \\ & x_{jk} \geq 0. \end{aligned} \tag{3.5}$$

Note that the solution satisfies  $x_{jk} \leq \min\{s_j, d_k\}$  since one cannot move more than  $s_j$  from any source vertex  $j$  and it is useless to bring more than  $d_k$  to any sink vertex  $k$ . From (3.5) it is easy to recover a standard LP problem

$$\begin{aligned} \text{minimize} \quad & \mathbf{c}^\top \mathbf{x} \\ \text{subject to} \quad & \mathbf{A}\mathbf{x} = \mathbf{b} \\ & \mathbf{x} \geq 0, \end{aligned} \tag{3.6}$$

simply defining

$$\mathbf{x} := (x_{11}, x_{12}, \dots, x_{1n}, x_{21}, x_{22}, \dots, x_{2J}, \dots, x_{J1}, \dots, x_{JJ})^\top \tag{3.7}$$

$$\mathbf{c} := (c_{11}, c_{12}, \dots, c_{1J}, c_{21}, c_{22}, \dots, c_{2J}, \dots, c_{J1}, \dots, c_{JJ})^\top \tag{3.8}$$

$$\mathbf{b} := (s_1, \dots, s_J, d_1, \dots, d_J)^\top \tag{3.9}$$

$$(3.10)$$

and  $\mathbf{A}$  as the  $2J \times J^2$  sparse matrix defined as

$$\mathbf{A} := \begin{bmatrix} \mathbb{1}_J & 0 & 0 & \cdots & 0 \\ 0 & \mathbb{1}_J & 0 & \cdots & 0 \\ 0 & 0 & \mathbb{1}_J & \cdots & 0 \\ \vdots & \vdots & \vdots & \ddots & \vdots \\ 0 & 0 & 0 & \cdots & \mathbb{1}_J \\ I_J & I_J & I_J & I_J & I_J \end{bmatrix} \quad (3.11)$$

where  $I_J$  is the  $J \times J$  identity matrix and  $\mathbb{1}_J := (\underbrace{1 \ 1 \ \cdots \ 1}_{J \text{ times}})$ .

### Error analysis

Before focusing on the sensitivity analysis of the LWR model, it is important to quantify the error introduced by the LP-based method presented above in computing the exact Wasserstein distance and then verify that this method is sufficiently accurate to our purposes.

**Proposition 3.1.** *Let  $\rho^s, \rho^d : \mathcal{N} \rightarrow \mathbb{R}$  two densities defined on a network  $\mathcal{N}$  such that*

$$M = \int_{\mathcal{N}} \rho^s dx = \int_{\mathcal{N}} \rho^d dx.$$

*Then,*

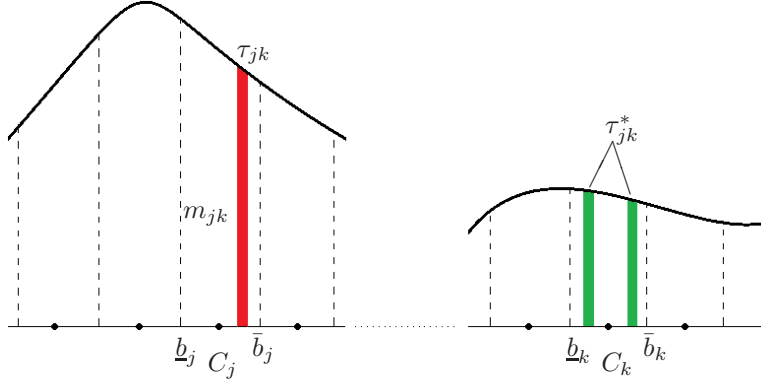
$$|W(\rho^s, \rho^d) - \mathcal{H}(\rho^s, \rho^d)| \leq M \Delta x. \quad (3.12)$$

**Proof.** To begin with, let us focus on a generic cell  $C_j$  of the network. In accordance with the optimal flow (found as the solution of the optimal mass problem), the mass in  $C_j$  is transferred in one or more cells of the network. Let us denote by  $m_{jk}$  the mass which is moved from cell  $C_j$  to  $C_k$  for some  $k = 1, \dots, J$  (including  $k = j$ ). Let us also denote by  $\tau_{jk}(\cdot)$  the density profile (with  $\text{supp}(\tau_{jk}) \subseteq C_j$ ) associated to the leaving mass  $m_{jk}$  in  $C_j$  and by  $\tau_{jk}^*(\cdot)$  the density profile (with  $\text{supp}(\tau_{jk}^*) \subseteq C_k$ ) associated to the arriving mass in  $C_k$ , see Fig. 6. By definition we have

$$m_{jk} = \int_{C_j} \tau_{jk}(x) dx = \int_{C_k} \tau_{jk}^*(x) dx.$$

Let us denote by  $\bar{b}_j := x_{j+\frac{1}{2}}$ ,  $\underline{b}_j := x_{j-\frac{1}{2}}$  and similarly by  $\bar{b}_k$ ,  $\underline{b}_k$  the two border points of the cell  $j$  and  $k$ , respectively. By suitably accumulating the masses at the *borders* of the cells, and recalling that the Hitchcock's approach requires instead to accumulate the masses at the *centres* of the cells, we have

$$W(\tau_{jk}, \tau_{jk}^*) \leq m_{jk} \max_{\substack{b_j \in \{\bar{b}_j, \underline{b}_j\} \\ b_k \in \{\bar{b}_k, \underline{b}_k\}}} W(\delta_{b_j}, \delta_{b_k}) = \mathcal{H}(\tau_{jk}, \tau_{jk}^*) + 2 \frac{m_{jk} \Delta x}{2},$$

Fig. 6. Theorem 3.1. Mass  $m_{jk}$  moving from  $C_j = [\underline{b}_j, \bar{b}_j]$  to  $C_k = [\underline{b}_k, \bar{b}_k]$ .

and, equivalently,

$$W(\tau_{jk}, \tau_{jk}^*) \geq m_{jk} \min_{\substack{b_j \in \{\bar{b}_j, \underline{b}_j\} \\ b_k \in \{\bar{b}_k, \underline{b}_k\}}} W(\delta_{b_j}, \delta_{b_k}) = \mathcal{H}(\tau_{jk}, \tau_{jk}^*) - 2 \frac{m_{jk} \Delta x}{2}$$

(where the additional distance  $\pm 2 \frac{m_{jk} \Delta x}{2}$  comes from moving the mass from the borders to the centres of the cells in  $C_j$  and  $C_k$ ). Summing up we obtain, by (3.5),

$$W(\rho^s, \rho^d) = \sum_j \sum_k W(\tau_{jk}, \tau_{jk}^*) \leq \sum_j \sum_k [\mathcal{H}(\tau_{jk}, \tau_{jk}^*) + m_{jk} \Delta x] = \mathcal{H}(\rho^s, \rho^d) + M \Delta x$$

and

$$W(\rho^s, \rho^d) = \sum_j \sum_k W(\tau_{jk}, \tau_{jk}^*) \geq \sum_j \sum_k [\mathcal{H}(\tau_{jk}, \tau_{jk}^*) - m_{jk} \Delta x] = \mathcal{H}(\rho^s, \rho^d) - M \Delta x.$$

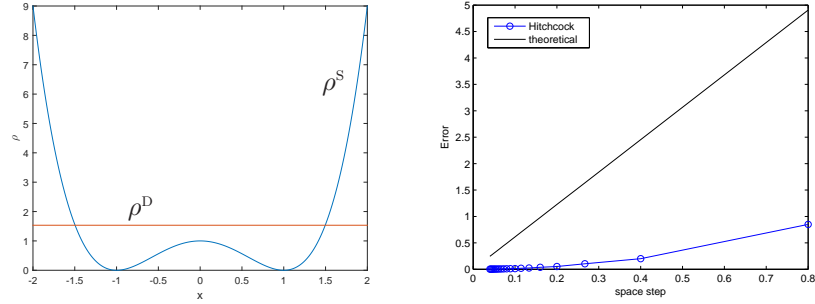
Finally we have

$$|W(\rho^s, \rho^d) - \mathcal{H}(\rho^s, \rho^d)| \leq M \Delta x. \quad \square$$

For a numerical confirmation of the result proved above, we ran a simple test on the real line to measure the convergence of the approximate Wasserstein distance as  $\Delta x \rightarrow 0$ . We define

$$\rho^s(x) = \begin{cases} x^4 - 2x^2 + 1, & x \in [-2, 2] \\ 0, & \text{otherwise} \end{cases}, \quad \rho^d(x) \equiv \frac{23}{15},$$

see Fig. 7(left). Note that the total mass is equal, i.e.  $M = \int_{\mathbb{R}} \rho^s = \int_{\mathbb{R}} \rho^d = \frac{92}{15}$ . The exact Wasserstein distance between the two densities can be easily computed by using (3.3), obtaining  $W(\rho^s, \rho^d) = 3.2$ . In Fig. 7(right) we report the value of the error  $|W - \mathcal{H}|$  as a function of the space step  $\Delta x$  used to discretise the interval  $[-2, 2]$ , and we compare it with the theoretical estimate given by Prop. 3.1. We note that the measured convergence rate is superlinear. This allows us to employ a relatively large space step  $\Delta x$  so as to keep within the limits the computational effort and memory storage for the LP problem.

Fig. 7. Functions  $\rho^S$  and  $\rho^D$  (left). Convergence of  $|W - H|$  as  $\Delta x \rightarrow 0$  (right).

### 3.3. Variational and PDE approach on networks

For the sake of completeness, and to promote further research in this area, we recall some other existing approaches to compute the Wasserstein distance on networks.

A recent paper by Mazón et al.<sup>22</sup> generalizes to networks the classical approach by Evans and Gangbo.<sup>11</sup> Let us define the functional

$$\mathcal{F}_p[u] := \frac{1}{p} \int_{\mathcal{N}} |u'(x)|^p dx - \int_{\mathcal{N}} u \, d(\nu^S - \nu^D) \quad (3.13)$$

with

$$u \in \mathcal{S}_p := \left\{ u \in W^{1,p}(\mathcal{N}) \text{ s.t. } \int_{\mathcal{N}} u(x) dx = 0 \right\}. \quad (3.14)$$

We have the following

**Lemma 3.1.** *Let  $u_p$  be a minimizer of the functional  $\mathcal{F}_p$  on  $\mathcal{S}_p$ ,  $p > 1$ . Then there exists a subsequence  $p_j \rightarrow \infty$  such that  $u_{p_j} \rightarrow u_\infty$  uniformly in  $\mathcal{N}$ . Moreover, the limit  $u_\infty$  is Lipschitz continuous and  $\|u'_\infty\|_{L^\infty(\mathcal{N})} \leq 1$ .*

The limit  $u_\infty$  is finally used to compute the Wasserstein distance

$$W_1(\nu^S, \nu^D) = \int_{\mathcal{N}} u_\infty \, d(\nu^S - \nu^D). \quad (3.15)$$

This approach can be indeed used to numerically compute the Wasserstein distance in simple cases, but it appears inadequate for complex networks. The reason is that a large exponent  $p$  in (3.13) requires a great precision in the approximation of the derivative which, in turn, raises the computational cost.

It can be also shown<sup>22</sup> that the minimizer  $u_p$  has a nice link with the  $p$ -Laplacian operator since it is a weak solution of the problem

$$\begin{cases} -(|u'|^{p-2} u')' = \nu^S - \nu^D, & \text{on edges,} \\ \sum_E \left| \frac{\partial u}{\partial x_E} \right|^{p-2} \frac{\partial u}{\partial x_E} = 0, & \text{on vertices.} \end{cases} \quad (3.16)$$

Observe that in the boundary condition in (3.16) the derivatives are taken in the direction away from the vertex. We have found also this PDE approach to be highly ill-conditioned for  $p \rightarrow \infty$ .

Finally, let us mention the method proposed in Ref. 26. The idea is to split the problem in three parts: first, the density distributed along the supplying edges is moved toward the adjacent vertices. Second, mass is optimally redistributed strictly on the vertex set as in a discrete graph. Third, the mass accumulated at vertices is dispersed along the demanding edges. This algorithm is exact (no discretisation error is introduced) but it raises complexity and CPU time.

#### 4. Sensitivity analysis

In this section we employ the Hitchcock approach described in Sec. 3.2 to perform a sensitivity analysis of the LWR model. Although the Hitchcock method is time consuming, it behaves well and does not introduce errors other than the ones related to the network discretisation (by the way, unavoidable in the numerical solution of the associated LWR model). To solve the LP problem we used the GLPK<sup>b</sup> free C library.

For numerical tests we considered the ‘‘Manhattan’’-like two-way road network depicted in Fig. 8. This choice is motivated by the fact that it allows one to easily compare networks of different size. Given the number  $\ell$  of junctions per side, we get  $\ell(\ell - 1)$  roads for each direction ( $4\ell(\ell - 1)$  roads total), and  $\ell^2$  junctions. Roads are numbered starting from those going rightward, then leftward, upward, and finally downward. The length of each road is  $L_E = 1$  and  $\Delta x = 0.1$  ( $J_E = 10$ ,  $J = 40\ell(\ell - 1)$ ).

In order to fairly compare simulations with different number of vehicles, we report the *normalized* (Hitchcock-approximate) Wasserstein distance

$$\hat{\mathcal{H}} := \frac{\sum_j \sum_k c_{jk} x_{jk}^*}{M},$$

where  $M = \sum_j s_j = \sum_j d_j$ , and  $x_{jk}^*$  is the solution of the LP problem (3.6).

##### 4.1. Sensitivity to the (positions of) initial data

In this test we measure the sensitivity to the position of initial density. The goal is to quantify the impact of a possible error in locating vehicles at initial time (but still catching the correct amount of vehicles).

The parameters which remain fixed in this test are

- *Fundamental diagram:*  $\sigma = 0.3$  and  $f_{\max} = 0.25$  (see (1.2)).
- *Distribution matrix:*

$$\alpha_{RR'}^V = \frac{1}{n_{\text{out}}^V}, \quad \forall V \in \mathcal{V}, \quad R = 1, \dots, n_{\text{inc}}^V, \quad R' = 1, \dots, n_{\text{out}}^V.$$

<sup>b</sup><https://www.gnu.org/software/glpk/>

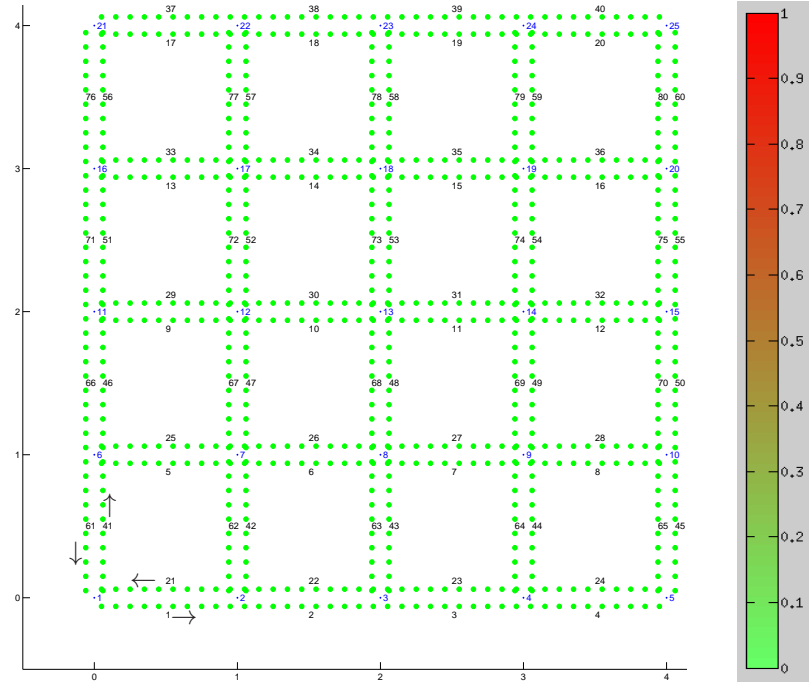


Fig. 8. Manhattan-like road network with  $\ell = 5$ . We report the numbering of roads and junctions. Roads are actually two-way, the small gap between lanes going in opposite directions is left for visualization purpose only.

#### 4.1.1. Case a (wrong support)

We consider the following two initial conditions, see Fig. 9: for all  $E \in \mathcal{E}$  and  $j = 1, \dots, J_E$ ,

$$\rho_{E,j}^{S,0} = \begin{cases} 0.8 & \text{for } 0 \leq j < 3 \\ 0 & \text{otherwise,} \end{cases} \quad \rho_{E,j}^{D,0} = \begin{cases} 0.4 & \text{for } 0 \leq j < 6 \\ 0 & \text{otherwise.} \end{cases} \quad (4.1)$$

From Fig. 10 we see that the distance between the corresponding solutions converges to zero as  $t \rightarrow \infty$ . This is due to the fact that vehicles spread across the whole network and in the limit their density is constant regardless of the initial datum.

#### 4.1.2. Case b (wrong direction)

For all  $E \in \mathcal{E}$  and  $j = 1, \dots, J_E$ ,

$$\rho_{E,j}^{S,0} = \begin{cases} 0.5 & \text{on rightward roads} \\ 0 & \text{elsewhere,} \end{cases} \quad \rho_{E,j}^{D,0} = \begin{cases} 0.5 & \text{on leftward roads} \\ 0 & \text{elsewhere.} \end{cases} \quad (4.2)$$

Although the limit behaviour is analogous to case a, Fig. 11 shows that in this case

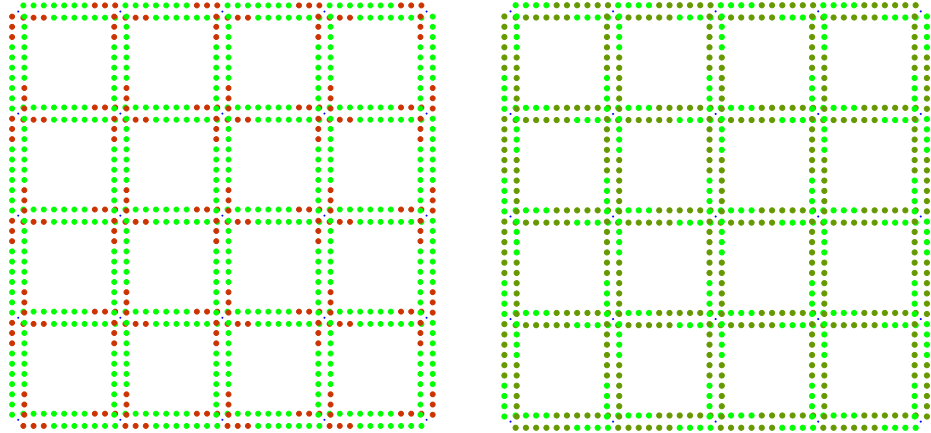


Fig. 9. Sensitivity to the initial density (case a).  $\ell = 5$  (80 roads). Initial datum  $\rho^{s,0}$  (left) and  $\rho^{d,0}$  (right).

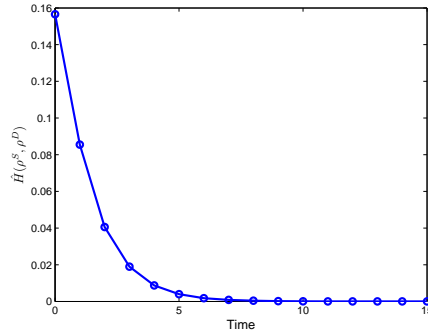


Fig. 10. Sensitivity to initial density (case a).  $\ell = 5$  (80 roads). Function  $t \rightarrow \hat{H}(\rho^s(\cdot, t), \rho^d(\cdot, t))$ .

the distance between the two solutions increases at the beginning. This is due to the fact that vehicles first move apart and then occupy the whole network. As expected, the size of the network affects the time scale, delaying the limit behaviour.

#### 4.2. Sensitivity to fundamental diagram

In this test we measure the sensitivity to the two parameters of the fundamental diagram, namely  $\sigma$  and  $f_{\max}$ . The goal is to quantify the impact of a possible error in measuring the capacity of the roads or in describing the drivers behaviour.

The parameters which remain fixed in this test are

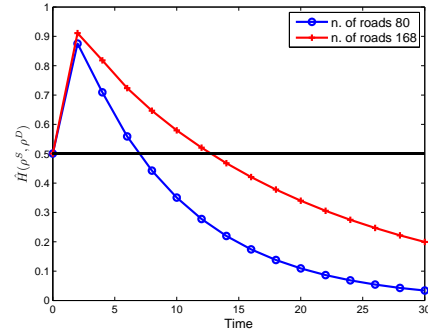


Fig. 11. Sensitivity to initial density (case b). Function  $t \rightarrow \hat{H}(\rho^s(\cdot, t), \rho^D(\cdot, t))$  for  $\ell = 5, 7$ .

- *Initial density:*

$$\rho_{E,j}^0 = \begin{cases} 0.5 & \text{on rightward roads,} \\ 0 & \text{elsewhere,} \end{cases} \quad E \in \mathcal{E}, \quad j = 1 \dots, J_E.$$

- *Distribution matrix:*

$$\alpha_{RR'}^V = \frac{1}{n_{\text{out}}^V}, \quad \forall V \in \mathcal{V}, \quad R = 1, \dots, n_{\text{inc}}^V, \quad R' = 1, \dots, n_{\text{out}}^V.$$

In Fig. 12 we report the distance between two solutions at final time  $T = 20$  obtained with  $f_{\max} = 0.25$ ,  $\sigma^s = 0.3$ , as a function of  $\sigma^D \in [0.15, 0.5]$  (left), and  $\sigma = 0.3$ ,  $f_{\max}^s = 0.25$ , as a function of  $f_{\max}^D \in [0.15, 0.4]$  (right). Errors in the

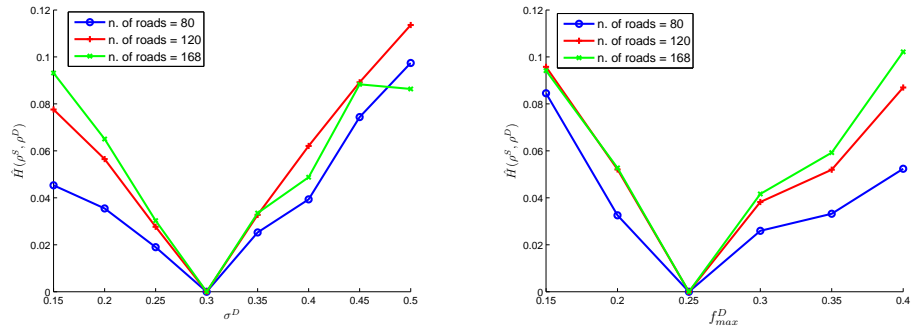


Fig. 12. Sensitivity to fundamental diagram. Function  $\sigma^D \rightarrow \hat{H}(\rho^s(\cdot, T), \rho^D(\cdot, T))$  (left) and,  $f_{\max}^D \rightarrow \hat{H}(\rho^s(\cdot, T), \rho^D(\cdot, T))$ , for  $\ell = 5, 6, 7$ .

calibration of  $\sigma$  or  $f_{\max}$  lead to similar discrepancies, which are again amplified by the network size. Discrepancies grow approximately linearly with respect to both  $|\sigma^D - \sigma^s|$  and  $|f_{\max}^D - f_{\max}^s|$ .

In Fig. 13 we report the distance between two solutions obtained with  $f_{\max} = 0.25$ ,  $\sigma^s = 0.3$ ,  $\sigma^D = 0.2$  (left), and  $\sigma = 0.3$ ,  $f_{\max}^s = 0.25$ ,  $f_{\max}^D = 0.3$  (right), as a function of time. Again, we see that the distances tend to 0 as  $t \rightarrow \infty$  because

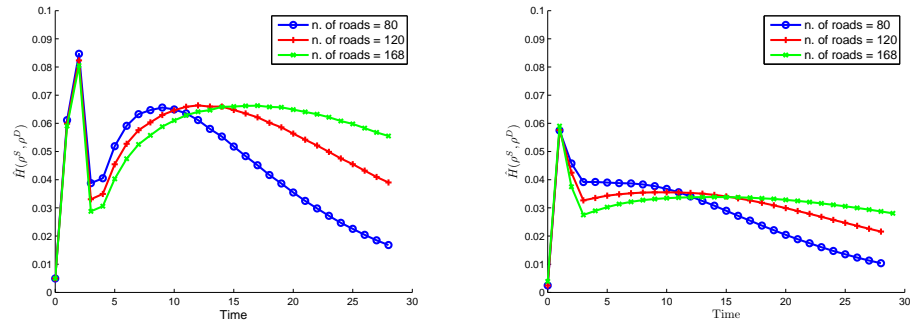


Fig. 13. Sensitivity to fundamental diagram. With respect to  $\sigma$  (left) and  $f_{\max}$  (right). Function  $t \rightarrow \hat{H}(\rho^s(\cdot, t), \rho^D(\cdot, t))$  for  $\ell = 5, 6, 7$ .

vehicles spread across the networks toward a stationary configuration and the size of the network affects the time scale.

The choice of a Manhattan-like network like the one depicted in Fig. 8 arises some doubts about the possible loss of generality, being that network perfectly regular. In order to have some insights about the sensitivity on a generic network, we run again the last test after closing three roads, thus breaking the symmetry. In more detail, we assume that roads 29, 58, and 61 (see Fig. 8), empty at  $t = 0$ , are closed immediately after the beginning of the simulation so that no one can enter there. In addition, the optimal mass transport problem is solved by preventing the mass to pass through the closed road. In Fig. 14 we report the results. We see that

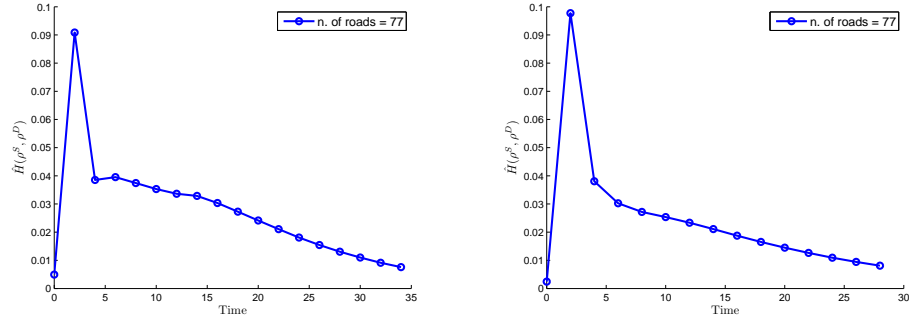


Fig. 14. Sensitivity to fundamental diagram. With respect to  $\sigma$  (left) and  $f_{\max}$  (right). Function  $t \rightarrow \hat{H}(\rho^s(\cdot, t), \rho^D(\cdot, t))$  for  $\ell = 5$  (three roads closed).

the behaviour is not dramatically different, and the distances still tend to 0, being the asymptotic solution equal (but not constant) for every choice of the parameters.

#### 4.3. Sensitivity to the distribution matrix

In this test we measure the sensitivity to the distribution coefficients at junctions, see Sec. 2.2. The goal is to quantify the impact of a possible error in the knowledge of the path choice at junctions.

The parameters which remain fixed in this test are

- *Initial density:*  $\rho_{E,j}^0 = 0.5$ ,  $E \in \mathcal{E}$ ,  $j = 1, \dots, J_E$ .
- *Fundamental diagram:*  $\sigma = 0.3$  and  $f_{\max} = 0.25$ .

Supply distribution  $\rho^S$  is obtained by means of equidistributed coefficients

$$\alpha_{RR'}^{S,V} = \frac{1}{n_{\text{out}}^V}, \quad \forall V \in \mathcal{V}, \quad R = 1, \dots, n_{\text{inc}}^V, \quad R' = 1, \dots, n_{\text{out}}^V.$$

Note that, due to the symmetry of the network and the initial datum,  $\rho^S \equiv 0.5$  for all  $x$  and  $t$ .

Demand distribution  $\rho^D$  is instead obtained by varying the distribution coefficients at the junction  $\bar{V}$  located at the very centre of the network (see, e.g., vertex 13 in Fig. 8). Variation is performed by means of a scalar parameter  $\varepsilon > 0$ . We have, for  $R = 1, 2, 3, 4$ ,

$$\alpha_{R1}^{D,\bar{V}} = \frac{1}{n_{\text{out}}^V} + \varepsilon, \quad \alpha_{R2}^{D,\bar{V}} = \frac{1}{n_{\text{out}}^V} - \varepsilon, \quad \alpha_{R3}^{D,\bar{V}} = \frac{1}{n_{\text{out}}^V} + \varepsilon, \quad \alpha_{R4}^{D,\bar{V}} = \frac{1}{n_{\text{out}}^V} - \varepsilon.$$

In Fig. 15 we report the distribution  $\rho^D$  at time  $t = 5$  and  $t = 15$  obtained with  $\varepsilon = 0.1$ , to be compared with the constant distribution. Remarkably, a minor local

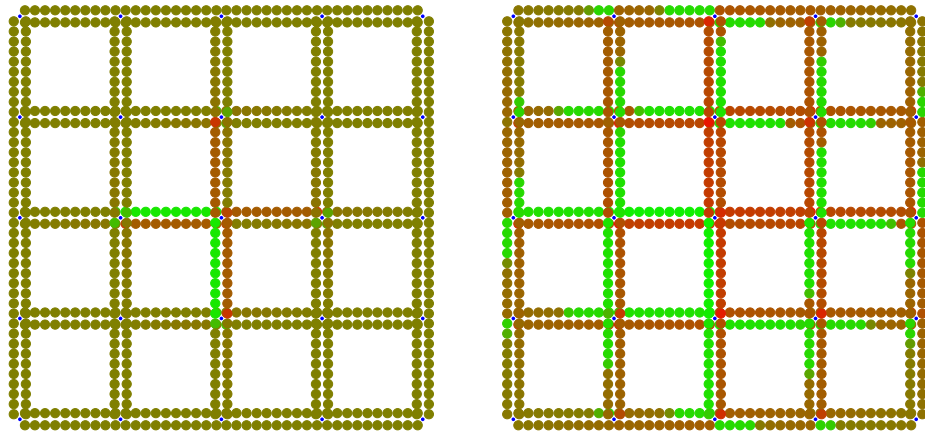


Fig. 15. Sensitivity to distribution matrix. Density  $\rho^D$  at time  $t = 5$  (left) and  $t = 15$  (right).

modification of the traffic distribution in a single junction breaks the symmetry and

has a great impact in the solution. This time the density does not tend to distribute uniformly and then we expect the distance  $W(\rho^D, \rho^S)$  to increase in time, although the growth cannot continue indefinitely since the distance between two distributions is finite on a finite network.

In Fig. 16 we show the distance between the two densities as a function of time for  $\varepsilon = 0.1, 0.2$ . The distance is indeed increasing, and tends to a limit value. A larger  $\varepsilon$  accelerates the process and let the distance reach the limit behaviour in shorter time. The impact of the network size is opposite with respect to the previous tests, being the smallest network the one with the greatest difference. This

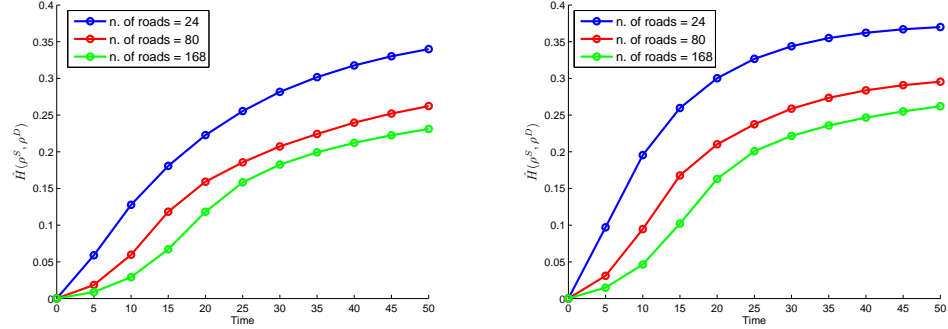


Fig. 16. Sensitivity to traffic distribution at junctions. Function  $t \rightarrow \hat{H}(\rho^S(\cdot, t), \rho^D(\cdot, t))$  for  $\ell = 3, 5, 7$ .  $\varepsilon = 0.1$  (left),  $\varepsilon = 0.2$  (right).

behaviour is going to change if we modify *all* the distribution coefficients, and not only those at one junction. In the following test we set, for any  $v$  and  $r = 1, 2, 3, 4$ ,

$$\alpha_{r1}^{D,V} = \frac{1}{n_{out}^v} + \varepsilon, \quad \alpha_{r2}^{D,V} = \frac{1}{n_{out}^v} - \varepsilon, \quad \alpha_{r3}^{D,V} = \frac{1}{n_{out}^v} + \varepsilon, \quad \alpha_{r4}^{D,V} = \frac{1}{n_{out}^v} - \varepsilon,$$

if  $v$  is labelled by an even number and

$$\alpha_{r1}^{D,V} = \frac{1}{n_{out}^v} - \varepsilon, \quad \alpha_{r2}^{D,V} = \frac{1}{n_{out}^v} + \varepsilon, \quad \alpha_{r3}^{D,V} = \frac{1}{n_{out}^v} - \varepsilon, \quad \alpha_{r4}^{D,V} = \frac{1}{n_{out}^v} + \varepsilon,$$

otherwise (at border junctions only the first two incoming roads  $r = 1, 2$  are considered). Results are shown in Fig. 17. After a transient, the sensitivity becomes proportional to the network size.

#### 4.4. Sensitivity to road network

In this test we measure the sensitivity to the road network. The goal is to quantify the impact of a possible change in the network, especially a road closure.

The parameters which remain fixed in this test are

- Initial density:  $\rho_{E,j}^0 = 0.3$ ,  $E \in \mathcal{E}$ ,  $j = 1, \dots, J_E$ .

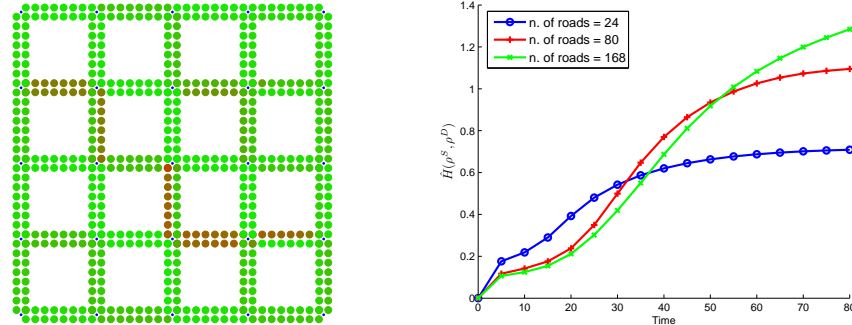


Fig. 17. Sensitivity to traffic distribution at junctions. Density  $\rho^D$  at time  $t = 20$  (left) and function  $t \rightarrow \hat{H}(\rho^s(\cdot, t), \rho^D(\cdot, t))$  for  $\ell = 3, 5, 7$  (right).

- *Fundamental diagram*:  $\sigma = 0.3$  and  $f_{\max} = 0.25$ .
- *Distribution matrix*: equidistributed along outgoing roads.

Supply distribution  $\rho^s$  is obtained solving the equations on the complete network, while demand distribution  $\rho^D$  is obtained by closing the central rightward road  $\bar{E}$  (see, e.g., edge 11 in Fig. 8) just after the initial time, i.e. vehicles can come out of the road but none of them can enter. Note that, due to the symmetry of the network and the initial datum,  $\rho^s \equiv 0.3$  for all  $x$  and  $t$ .

In Fig. 18(left) we report the distribution  $\rho^D$  at time  $t = 10$ , to be compared with the constant distribution. Similarly to the previous test, a local modification

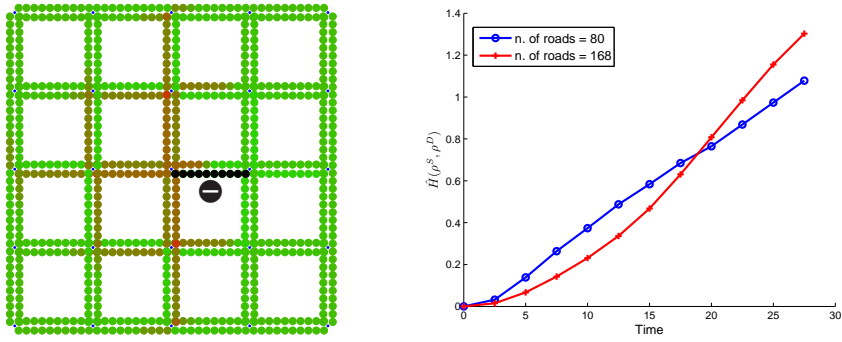


Fig. 18. Sensitivity to road network. Density  $\rho^D$  at time  $t = 10$  (left) and function  $t \rightarrow \hat{H}(\rho^s(\cdot, t), \rho^D(\cdot, t))$  for  $\ell = 5, 7$  (right).

of the network breaks the symmetry and has a great impact in the solution. In Fig. 18(right) we show the distance between the two densities as a function of time. The behaviour with respect to the network size is similar to that shown in Fig. 17(right),

where the long-time behaviour of the sensitivity is proportional to the network size, even if here the road closure has only a local (but stronger) impact.

## 5. Conclusions

In this paper we have studied the impact of various sources of error on the final output of the LWR model on large networks. The difference between two solutions was evaluated by means of the Wasserstein distance between the two. The numerical computation of the Wasserstein distance was obtained by recasting the problem into the optimal mass transfer framework and recovering a standard LP problem. The Wasserstein distance is indeed confirmed to be the right notion of distance to be used in this context, being able to catch the differences among distribution in a regular and smooth fashion. Unfortunately, its numerical approximation on spaces other than the real line is not trivial. The LP-based method here proposed seems to be appropriate although the computational cost and memory requirements increase nonlinearly with the number of grid nodes.

Wrong estimation of the position of vehicles at initial time does not seem to have a major impact on the final solution, at least for large times and small networks. Similar conclusions apply to wrong estimation of the fundamental diagram: errors on  $\sigma$  or  $f_{\max}$  have approximately the same impact on the final solution, and the discrepancy grows approximately linearly with respect to both  $|\sigma^D - \sigma^S|$  and  $|f_{\max}^D - f_{\max}^S|$ .

Conversely, wrong estimation of traffic distribution at junctions seems to have a far greater impact. Vehicles are redirected in the wrong direction at every passage across the junction, therefore the error grows as the time goes by. Neglecting a road closure has basically the same effect since vehicles are redistributed along closest roads. It is likely that in real situation the estimation of all distribution coefficients are inaccurate. In this case the error grows with the network size and the prevision can become rapidly unusable.

Interestingly, last tests show that the network size can either amplify or reduce the effect of local changes on parameters. Further studies could be dedicated to measure the impact of local modifications on the global dynamics.

## Acknowledgements

Authors want to thank Sheila Scialanga for the help in writing the numerical code and testing other than Wasserstein distances. Authors also thank Fabio Camilli and Simone Cacace for the useful discussions and wrong suggestions.

## References

1. N. Bellomo and C. Dogbe, *On the modeling of traffic and crowds: A survey of models, speculations, and perspectives*, SIAM Rev., **53** (2011), 409–463.
2. F. Bolley, Y. Brenier and G. Loeper, Contractive metrics for scalar conservation laws, *Journal of Hyperbolic Differential Equations* **2** (2005) 91–107.

3. A. Bressan and K. T. Nguyen, Conservation law models for traffic flow on a network of roads, *Netw. Heterog. Media* **10** (2015) 255–293.
4. G. Bretti, M. Briani and E. Cristiani, An easy-to-use algorithm for simulating traffic flow on networks: numerical experiments, *Discrete Contin. Dyn. Syst. Ser. S* **7** (2014) 379–394.
5. M. Briani and E. Cristiani, An easy-to-use algorithm for simulating traffic flow on networks: theoretical study, *Netw. Heterog. Media* **9** (2014) 519–552.
6. G. M. Coclite, M. Garavello and B. Piccoli, Traffic flow on a road network, *SIAM J. Math. Anal.* **36** (2005) 1862–1886.
7. E. Cristiani, B. Piccoli and A. Tosin, *Multiscale Modeling of Pedestrian Dynamics*, Modeling, Simulations & Applications **12** (Springer, 2014).
8. E. Cristiani and F. S. Priuli, A destination-preserving model for simulating Wardrop equilibria in traffic flow on networks, *Netw. Heterog. Media* **10** (2015) 857–876.
9. E. Cristiani and S. Sahu, On the micro-to-macro limit for first-order traffic flow models on networks, *Netw. Heterog. Media* **11** (2016). In press.
10. M. Di Francesco and M. D. Rosini, Rigorous derivation of nonlinear scalar conservation laws from follow-the-leader type models via many particle limit, *Arch. Rational Mech. Anal.*, **217** (2015) 831–871.
11. L. C. Evans and W. Gangbo, Differential equations methods for the Monge–Kantorovich mass transfer problem, *Mem. Amer. Math. Soc* **137** No. 653 (1999).
12. U. S. Fjordholm and S. Solem, Second-order convergence of monotone schemes for conservation laws, *SIAM J. Numer. Anal.* **54**, 1920–1945.
13. M. Garavello and P. Goatin, The Cauchy problem at a node with buffer, *Discrete Contin. Dyn. Syst. Ser. A*, **32** (2012) 1915–1938.
14. M. Garavello and B. Piccoli, *Traffic Flow on Networks*, AIMS on Applied Math. **1** (American Institute of Mathematical Sciences, 2006).
15. M. Garavello and B. Piccoli, A multibuffer model for LWR road networks, Advances in Dynamic Network Modeling in Complex Transportation Systems, Complex Networks and Dynamic Systems, Vol. 2, 2013, 143–161.
16. R. Haberman, *Mathematical Models: Mechanical Vibrations, Population Dynamics and Traffic Flow*, (Prentice-Hall, Inc., Englewood Cliffs, New Jersey, USA, 1977).
17. D. Helbing, Traffic and related self-driven many-particle systems, *Rev. Modern Phys.*, **73** (2001) 1067–1141.
18. M. Herty, J.-P. Lebacque and S. Moutari, A novel model for intersections of vehicular traffic flow, *Netw. Heterog. Media* **4** (2009) 813–826.
19. M. Hilliges and W. Weidlich, A phenomenological model for dynamic traffic flow in networks, *Transportation Research Part B* **29** (1995) 407–431.
20. H. Holden and N. H. Risebro, A mathematical model of traffic flow on a network of unidirectional roads, *SIAM J. Math. Anal.* **26** (1995) 999–1017.
21. M. J. Lighthill and G. B. Whitham, On kinetic waves. II. Theory of traffic flows on long crowded roads, *Proc. Roy. Soc. Lond. A* **229** (1955) 317–345.
22. J. M. Mazón, J. D. Rossi and J. Toledo, Optimal mass transport on metric graphs, *SIAM J. Optim.* **25** (2015) 1609–1632.
23. H. Nessyahu and E. Tadmor, The convergence rate of approximate solutions for nonlinear scalar conservation laws, *SIAM J. Numer. Anal.* **29** (1992) 1505–1519.
24. P. I. Richards, Shock waves on the highway, *Operations Res.* **4** (1956) 42–51.
25. S. M. Sinha, *Mathematical Programming: Theory and Methods* (Elsevier Science & Technology Books, 2006).
26. K. Treleaven and E. Frazzoli, Computing Earth Movers Distances on a road map with applications to one-way vehicle sharing, 2014 American Control Conference (ACC),

24 *M. Briani, E. Cristiani & E. Iacomini*

June 4-6, 2014. Portland, Oregon, USA.

27. C. Villani, *Optimal Transport: Old and New* (Springer, 2009).